Pacific Symposium on Biocomputing 25:355-366(2020)

PAGE-Net: Interpretable and Integrative Deep Learning for Survival Analysis Using Histopathological Images and Genomic Data

Jie Hao[1*], Sai Chandra Kosaraju[2*], Nelson Zange Tsaku[3], Dae Hyun Song[4], and Mingon Kang[2]

[1]*Department of Biostatistics, Epidemiology and Informatics, University of Pennsylvania, Philadelphia, PA, USA*

[2]*Department of Computer Science, University of Nevada Las Vegas, Las Vegas, NV, USA*

[3]*Department of Computer Science, Kennesaw State University, Marietta, GA, USA*

[4]*Department of Pathology, Gyeongsang National University Changwon Hospital, Changwon, Republic of Korea*

** Authors contributed equally*

Corresponding authors: mingon.kang@unlv.edu

The integration of multi-modal data, such as histopathological images and genomic data, is essential for understanding cancer heterogeneity and complexity for personalized treatments, as well as for enhancing survival predictions in cancer study. Histopathology, as a clinical gold-standard tool for diagnosis and prognosis in cancers, allows clinicians to make precise decisions on therapies, whereas high-throughput genomic data have been investigated to dissect the genetic mechanisms of cancers. We propose a biologically interpretable deep learning model (PAGE-Net) that integrates histopathological images and genomic data, not only to improve survival prediction, but also to identify genetic and histopathological patterns that cause different survival rates in patients. PAGE-Net consists of pathology/genome/demography-specific layers, each of which provides comprehensive biological interpretation. In particular, we propose a novel patch-wise texture-based convolutional neural network, with a patch aggregation strategy, to extract global survival-discriminative features, without manual annotation for the pathology-specific layers. We adapted the pathway-based sparse deep neural network, named Cox-PASNet, for the genome-specific layers. The proposed deep learning model was assessed with the histopathological images and the gene expression data of Glioblastoma Multiforme (GBM) at The Cancer Genome Atlas (TCGA) and The Cancer Imaging Archive (TCIA). PAGE-Net achieved a C-index of 0.702, which is higher than the results achieved with only histopathological images (0.509) and Cox-PASNet (0.640). More importantly, PAGE-Net can simultaneously identify histopathological and genomic prognostic factors associated with patients survivals. The source code of PAGE-Net is publicly available at `https://github.com/DataX-JieHao/PAGE-Net`.

Keywords: Survival Analysis; TCGA; TCIA; Data Integration; Integrative Deep Learning.

1. Introduction

The integration of histopathological images and genomic data has enhanced personalized treatments and survival predictions in cancer study, while providing an in-depth understanding of both the phenotypic patterns and genetic mechanisms of cancer.[1,2] Histopathological

images encompass rich phenotypic information with respect to tumor morphology, and high-throughput genomic data have unveiled the molecular profiles of cancer.[3] Histopathology, as a clinical gold standard tool in the diagnosis and prognosis of most cancers, allows clinicians to make precise decision on therapies.[4] Along with the advance of technology in microscopy, digital Whole Slide Imaging (WSI) enables pathologists to manage histopathological tissue slides efficiently. However, manual assessments with large-scale histopathological images are highly time-consuming and subjective, especially by pathologists who have varying levels of experience.

An increasing number of methods have been developed to leverage machine learning techniques for the automatic classification of cancer subtypes, identification of metastases, and nuclei segmentation for pathological image analysis.[5] Deep learning techniques, especially convolutional neural networks (CNNs), have shown tremendous potential in automatic histopathological image analysis. A deep max-pooling CNN was applied for mitosis detection in breast cancer histological images.[6] Transfer learning-based deep convolutional activation features were extracted to classify glioma grades and to segment the presence of necrosis in Glioblastoma Multiforme (GBM), where ImageNet was adopted for a pre-trained model.[7] An ensemble of CNNs was developed to imporve the predictive performance of tumor grades.[8] In the ensemble, a CNN classified high and low-grade glioma, and another CNN further differentiated the grade level in low-grade glioma only. An automatic recognition of nine important nuclear morphological characteristics in pathological images of glioma were constructed by a semi-supervised CNN and a pre-trained CNN (i.e. VGG16) with Support Vector Machine (SVM).[9]

Survival analysis aims to estimate an expected survival time, until a death event occurs. More importantly, a cancer survival model investigates the prognostic factors associated to a cancer. The Cox proportional hazards model and its variants are the most commonly applied in medical research. However, the conventional Cox model assumes a linear relationship of covariates, which is rarely applied to complex diseases without feature selection of high-dimensional data.

Deep learning-based Cox regressions, with histopathological images, have been studied to tackle the problems of non-linearity and multi-collinearity between covariates. Survival Convolutional Neural Networks (SCNNs) were developed to predict patient survival outcomes by high-power fields (HPFs) from Regions Of Interests (ROIs) that show morphological patterns, with representative tumor characteristics.[10] A Whole Slide Histopathological Images Survival Analysis framework (WSISA) was proposed to directly learn discriminative patches, based on cluster-level Deep Convolutional Survival (DeepConvSur) models for predicting patient survival.[11] The study introduced an aggregation strategy based on the weighted features evaluated by the performance in each cluster.

Recently, the integration of histopathological and genomic data has been explored as a promising solution for predicting cancer survival outcomes. A lasso-regularized Cox proportional hazards model extracted pre-defined morphological features from digital WSIs and eigen-genes from gene co-expression data in clear cell renal cell carcinoma, and outperformed the models with either morphological features or eigen-genes individually.[1] A multiple kernel

learning-based method was introduced to extract heterogeneous features from multiple types of genomic data and pathological images in breast cancer.[12] Genomic Survival convolutional neural networks (GSCNN) integrated heterogeneous features from both pathological images and well-known genomic biomarkers for predicting patient survival with glioma.[10]

Although the integrative models have produced higher predictive performance than single data models for cancer survival, most integrative models require intensive data preprocessing, with manually annotated ROIs on histopathological images, and stringent feature selection to reduce the numbers of input features, e.g., using well-known genomic biomarkers from the biological literature. For instance, GSCNN integrated only two well-known genomic biomarkers with a pre-trained SCNN model in order to reduce the number of covariates and false negative prognostic factors.[10] Pre-defined image features of geometry, texture, and holistic statistics were extracted from Hematoxylin and Eosin (H&E) pathological slides, prior to integrating them with gene expression data.[2]

In this paper, we propose a biologically interpretable, integrative deep learning model that integrates histoPAthological images and GEnomic data, called PAGE-Net, not only to improve survival prediction, but also to identify genetic and histopathological patterns that may cause different survival rates between patients. The major methodological challenges when integrating unstructured mega-pixel histopathological images and structured genomic data are data heterogeneity and complexity. Our main contributions with PAGE-Net for cancer survival analysis are threefold: (1) to integrate histopathological images and genomic data in a biologically interpretable deep learning model; (2) to identify survival-discriminative features without manually annotated ROIs; and (3) to provide an aggregation strategy that aggregates patch-level features generated from multiple patches, and produces image-level global features.

2. Methods

2.1. *The architecture of PAGE-Net*

PAGE-Net consists of pathology-specific layers, genome-specific layers, and a demography-specific layer, each of which provide the interpretability of a biological mechanism, and histopathological patterns associated to cancer survival, as illustrated in Fig. 1. In order to tackle the integration challenge between an unstructured mega-pixel WSI and structured genomic data, we propose a novel patch-wise texture-based convolutional neural network with a patch aggregation strategy (described in Section 2.2 in detail) to extract survival-discriminative features, without manually annotated ROIs for the pathology-specific layers. First, survival-discriminative features are identified by a pre-trained deep learning model with uncensored data only. Then the feature scores are aggregated from multiple patches of a WSI, which generates structured vector data. For the genome-specific layers and the demography-specific layer, we adapt the previously proposed, pathway-based sparse deep neural network, named Cox-PASNet.[13] Cox-PASNet is a cutting-edge deep learning model that interprets biological mechanisms by incorporating gene expression data and clinical data, as well as prior biological knowledge of pathways, while holding outstanding predictive performance of patient survival, with high-dimension, low-sample size biological data. Finally, the high-level representations of the histopathologcial and genomic data, along with clinical information, are

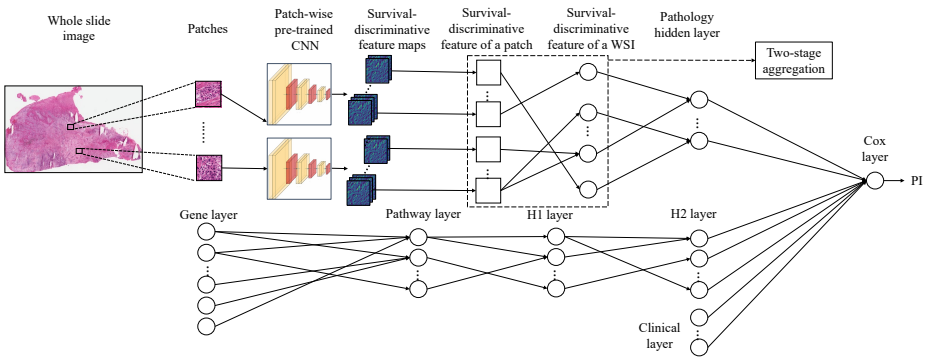

Fig. 1. The architecture of PAGE-Net

introduced to a shared layer that estimates the Prognostic Index (PI) in a Cox proportional-hazards regression model.

2.2. *Pathology-specific layers*

In the pathology-specific layers, survival-discriminative features, which are identified in advance by a pre-trained CNN, are extracted from multiple patches of a histopathologcial image. Then the features are aggregated by a two-stage pooling strategy and introduced to a Cox layer, along with the last hidden layer of the genome-specific layers, and the clinical layer. We elucidate the pre-trained CNN model and the aggregation strategy in the following subsections.

2.2.1. *Patch-wise pre-trained CNN*

We train a CNN model to identify survival-discriminative feature maps with patches from uncensored histopathologcial images, prior to the proposed integrative deep learning model. The histopathological patterns are captured by the pre-trained CNN, with dilated convolutional layers. Dilated convolutional layers enlarge the field-of-view (i.e. texture) without the loss of spatial information.[14] The number of parameters does not increase with dilation, which makes model training computationally efficient. Moreover, dilated convolutional layers trade off computational time against context assimilation.[15]

The pre-trained CNN model is comprised of an input layer, three pairs of dilated convolutional layers (a kernel size of 5×5, 50 feature maps, and a dilation rate of 2) and a max-pooling layer of 2×2 size. The sequential layers are followed by a flatten layer and a fully connected layer. We use a linear model as the output layer, since the model is trained with only uncensored data. Finally, the 50 neurons in the last max-pooling layer are considered as the survival-discriminative features in the integrative model. Fig. 2 illustrates the details of the pre-trained model.

2.2.2. *Two-stage aggregation*

Global survival-discriminative features for a WSI are generated by a two-stage pooling aggregation strategy. Each patch image produces N numbers of *local* survival-discriminative feature scores from the pre-trained CNN, and the scores of multiple patches from the WSI are aggregated. The aggregated scores are introduced into the last hidden layer in the pathology-specific

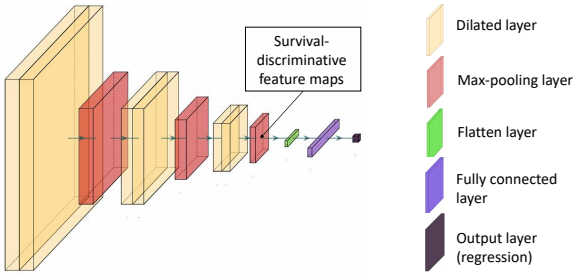

Fig. 2. The architecture of the pre-trained CNN

layers.

We adapt a two-stage pooling approach,[16] by computing 3-norm pooling, so that only a highly-ranked subset of patches is considered.[7,17] The first stage pooling ranks survival-discriminative features, and identifies the most important features. Then the second stage pooling forms global survival-discriminative features, by aggregating only top-ranked patches.

The first stage pooling: Suppose that there are N survival-discriminative feature maps identified by the pre-trained CNN on each patch image (i.e., 50 neurons in the last max-pooling layer of the pre-trained CNN in this study). Let $\mathbf{X}$ denote N survival-discriminative feature maps, where $\mathbf{X} = [\mathbf{X}_1, \mathbf{X}_2, \mathbf{X}_3, \ldots, \mathbf{X}_N]$. The i^{th} survival-discriminative feature map, $\mathbf{X}_i$ $(1 \leq i \leq N)$, can be represented as:

$$\mathbf{X}_i = \begin{bmatrix} x_{11} & x_{12} & x_{13} & \ldots & x_{1w} \\ x_{21} & x_{22} & x_{23} & \ldots & x_{2w} \\ \vdots & \vdots & \vdots & \ddots & \vdots \\ x_{h1} & x_{h2} & x_{h3} & \ldots & x_{hw} \end{bmatrix}, \tag{1}$$

where h and w are the height and the width of the feature map, respectively (e.g., $h = w = 18$ in this study). Then the flattened feature map becomes $\mathbf{X}_i^f = [x_{11}, x_{12}, x_{13}, \ldots, x_{hw}]$. After sorting the flattened feature map in descending order, the top K_1 features are considered as significant survival-discriminative feature map components, which are $\tilde{\mathbf{X}}_i^f = \tilde{x}_1, \tilde{x}_2, \tilde{x}_3, \ldots, \tilde{x}_{K_1}$. Then a 3-norm pooling value on $\tilde{\mathbf{X}}_i^f$ is computed by $f_i = \frac{1}{K_1}(\sum_{j=1}^{K_1}(\tilde{x}_j^f)^3)^{1/3}$, where f_i is an aggregated score for the i^{th} feature map on a patch.

The second stage pooling: Suppose that M numbers of patches are available on a WSI. The aggregated feature maps of all patches, after the first stage pooling, can be represented as:

$$\boldsymbol{F} = \begin{bmatrix} f_{11} & f_{12} & f_{13} & \ldots & f_{1N} \\ f_{21} & f_{22} & f_{23} & \ldots & f_{2N} \\ \vdots & \vdots & \vdots & \ddots & \vdots \\ f_{M1} & f_{M2} & f_{M3} & \ldots & f_{MN} \end{bmatrix}, \tag{2}$$

where f_{ij} is the j^{th} feature map of the i^{th} patch on a WSI. For each column of $\mathbf{F}$ (i.e. feature maps over M patches), column-wise values are sorted in descending order. The top K_2 number

of values (i.e. important patches) in each column are truncated, i.e., $\tilde{f}_{ij}, 1 \leq i \leq K_2$. Then another 3-norm pooling is performed on each column of the truncated $\mathbf{F}$. An aggregated score of the top K_2 discriminative patches is obtained for a feature map. Therefore, a vector of N aggregated survival-discriminative features represents a histopathologcial WSI for a patient. In this study, $N = 50$, $M = 1000$, $K_1 = 65$, and $K_2 = 100$ were used.

2.3. *Genome- and demography-specific layers*

The genome and demography-specific layers are adapted from the pathway-based sparse deep neural network, Cox-PASNet.[13] The genome-specific layers include a gene layer, a pathway layer, and two hidden layers (H1 and H2). The gene layer is an input layer for gene expression data, where each node indicates a gene. The pathway layer embeds prior biological knowledge, using well-known biological pathway databases (e.g., KEGG) for biological interpretation. The connection between the gene layer and the pathway layer are sparsely established by given biological pathway databases, where the relationships between genes and pathways are available. Hence, each pathway node explicitly represents a biological pathway. The following two hidden layers capture the nonlinear and hierarchical relationships between the pathways. Clinical patient data are directly introduced to the demography-specific layer, and combined with genomic features from gene expressions and aggregated survival-discriminative features from a histopathologcial image in the last hidden layer of the integrative model.

Overfitting is a critical issue to avoid when training a deep learning model with high-dimension, low-sample-size data. In order to prevent the overfitting problem, PAGE-Net applies the training technique that Cox-PASNet proposed.[13] Instead of training the whole network, small networks are randomly selected, and sparse coding is applied to make connections sparse for model interpretation. The training is repeated until it converges. Errors with the validation data are also traced for early stopping, and preventing overfitting.

3. Experimental Results

We examined the histopathologcial images, gene expression data, and clinical data of GBM patients to assess the proposed model. The data were downloaded from The Cancer Imaging Archive (TCIA) and The Cancer Genome Atlas (TCGA), which provide histopathologcial images and genomic data from an identical set of patients. We considered only GBM patients' data, where both gene expression and histopathologcial images were available. Additionally, samples without survival information were filtered out. Only age was included as a clinical feature for the demography-specific layer, i.e. clinical layer, since a large amount of missing values were shown in other clinical features.

KEGG and Reactome pathway databases, taken from the Molecular Signatures Database (MSigDB), were used as prior biological knowledge for the biological pathways in the model. Biological pathways that had either less than fifteen genes or over 300 genes were excluded.[18] Furthermore, only genes that belonged to at least one pathway were considered as inputs in the model. Finally, 5,404 genes of 447 GBM patients were considered, and 659 pathways were examined. For the histopathologcial WSI, we considered the WSIs of the "top" frozen tissue sections with 20X magnification. In the pre-training phase, 1,000 256×256 size patches were randomly sampled from the uncensored data for training the pre-trained CNN. Note

that only uncensored training and validation data were used for the pre-trained CNN in each experiment. In the integration phase, another 1,000 patches were sampled from a WSI for training and testing.

We compared the predictive performance of PAGE-Net with Cox-PASNet, and Cox regression with elastic net regularization (Cox-EN).[19] Cox-PASNet was applied to gene expressions and age, whereas aggregated survival-discriminative image features were trained by Cox-EN. A concordance index (C-index), which measures the concordance pairs (including tied pairs) between actual survival time and prediction risk scores, was used to evaluate the model performance. The C-index's range is between 0 and 1, where 1 is perfect prediction, and 0.5 is random guess. The samples were randomly split into training (80%), validation (10%), and test (10%) sets, by preserving the proportion between censored and uncensored status. The features in the training set were normalized to a mean of zero and standard deviation of one. The validation and test sets were normalized by the mean and standard deviation from the training set. We repeated the experiments 20 times to show the reproducibility of the performance.

PAGE-Net was implemented by PyTorch 1.0 with CUDA 10.0.130 and Keras 2.2.4 with TensorFlow 1.13.1 as a backend. The model was optimized with a dilated kernel size of 5×5, dilated rate r of 2, and max pooling size of 2×2. A dropout rate of 0.3 was applied for each dilated conventional layer and flatten layer. We used an Adaptive Moment Estimation (Adam) optimizer and an ReLU activation function. The mean squared error (MSE) was computed as the loss. A grid search was performed on each experiment to optimize the learning rate and a mini-batch size, using the validation data with a learning rate decay of 0.7 for every five epochs. Early stopping upon validation loss was applied.

In the integration phrase, a Tanh function was used as the activation function between layers. We set 100, 30, and 30 nodes for H1, H2, and the pathology hidden layer, respectively. Dropout rates were empirically set as 0.7, 0.5, and 0.3 for the pathway layer, H1, and the global survival-discriminative feature layer, respectively. The optimal learning rate and L^2 regularization (λ) were automatically determined by a grid search, so as to maximize the C-index with the validation data in each experiment. All experiments were performed with two NVIDIA Tesla M40 (8 cores, 12GB memory per each core) Graphics Processing Units (GPUs). The source code of PAGE-Net is accessible online via GitHub (`https://github.com/DataX-JieHao/PAGE-Net`). For the benchmark methods, Cox-PASNet was performed in the manner proposed in the paper. Cox-EN was implemented by the Python version of *Glmnet Vignette*.[19] Two-hundred λs were considered for optimization. The regularization term α between zero and one was optimized by a grid search with a step size of 0.01.

The experimental results with the GBM data are shown in Fig. 3. Our proposed model, PAGE-Net, achieved the highest C-index of 0.702 ± 0.0294 (mean ± std), compared to Cox-PASNet (with gene expressions and age) showing a C-index of 0.6401 ± 0.00399, and a Cox-EN (with aggregated image features) showing the lowest C-index of 0.5093 ± 0.0460. The highest C-index of PAGE-Net shows increased power of the integrative model with the histopathologcial data and genomic data. Interestingly, the histopathologcial WSI itself contributes little to the predictive performance. However, the experimental results show that the histopathologcial

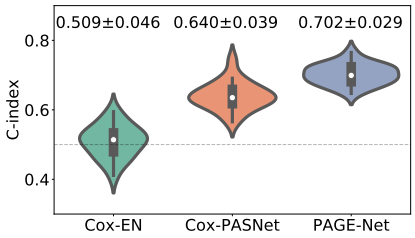

Fig. 3. Performance comparison over 20 experiments with GBM in C-index.

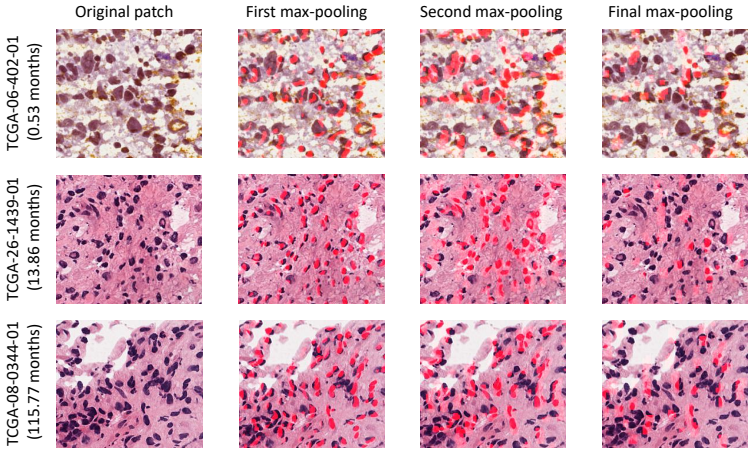

Fig. 4. Survival-discriminative feature maps on the patches of three patients at various survival rates.

WSI boosted the performance of the survival analysis with genomic data in the proposed integrative model. The performances were assessed by Wilconxon rank-sum tests; and PAGE-Net statistically outperformed Cox-EN with histopathologcial images only, and Cox-PASNet with genomic data only (both p-values are less than 0.0001).

4. Model Interpretation

For the model interpretation of PAGE-Net, we re-trained the proposed models using the entire dataset, as well as the optimal hyper-parameters that were the most commonly used over the 20 experiments. We performed an analysis for biological interpretation with the pathology and genome-specific layers. For the pathology-specific layers, histopathological patterns of the survival-discriminative feature maps were assessed with a pathologist. For the genome-specific layers, we conducted a pathway-based interpretation, by ranking the nodes with partial derivatives, as conducted by Cox-PASNet.[13]

Figure 4 exhibits the top-ranked histopathologcial patch images of three patients in short (first row; *TCGA-06-402-01*; survival month = 0.53), median (second row; *TCGA-26-1439-01*; survival month = 13.85), and long-term (third row; *TCGA-08-0344-01*; survival month = 115.3) survival rates, as well as the survival-discriminative feature maps captured by the pre-trained CNN on the patches. The survival-discriminative feature map scores (higher than the median) are colored in red in the figures. Interestingly, the survival-discriminative feature maps capture most nuclei and nuclear debris of interest on the patches. In GBM, where the

boundaries between nuclei are not clearly shown, a distance between nuclei and the shape of a nucleus are critical checkpoints on tissue readings. The feature maps show that the morphological patterns of interest to pathologists are also recognized by the proposed model. Moreover, nuclear debris implies the necrosis of a nucleus, and the relationship between nuclear debris and survival prognosis is known. The top-ranked patches were measured with scores of nuclear pleomorphism (NP), cytoplasmic degeneration (CD), and brown pigment (BP) using three tiered scoring by a pathologist. The scores of NP, CD, and BP on *TCGA-06-402-01* were +3, +3, and +3, respectively, whereas the scores of *TCGA-26-1439-01* and *TCGA-08-0344-01* were +1, 0, and 0, respectively. The patch of patient, *TCGA-06-402-01*, shows more severe scores on NP, CD, and BP than the other two patients. It shows that PAGE-Net can also identify regions (patches) associated with patient survival on a WSI.

Table 1. Ten top-ranked pathways in GBM by PAGE-Net

Pathway name	# of genes	P-value	References
Neuroactive ligand-receptor interaction	272	< 0.0001	20,21
Axon guidance	129	< 0.0001	22
Transmission across chemical synapses	186	< 0.0001	–
G alpha (s) signalling events	121	< 0.0001	–
Neuronal system	279	< 0.0001	–
Endocytosis	183	< 0.0001	23,24
Tyrosine metabolism	42	0.3924	–
Collagen formation	58	0.1041	25
Neurotransmitter receptor binding and downstream transmission in the postsynaptic cell	137	< 0.0001	–
Cytokine-cytokine receptor interaction	267	< 0.0001	26

Table 2. Ten top-ranked genes in GBM by PAGE-Net

Gene name	P-value	References	Gene name	P-value	References
PTGER4	0.5679	27	ADORA2A	0.0064	28
NPY2R	0.0358	_	MET	0.0066	29
LHB	0.1379	_	FSHB	0.0330	_
GHRHR	0.0578	30	HTR7	0.8468	31
ADRB3	0.0217	_	GRM8	0.6673	32

The ten top-ranked pathways and genes in GBM are ranked with genome-specific layers in PAGE-Net. The pathways and genes are listed in Table 1 and Table 2. The neuroactive ligand-receptor interaction pathway, ranked as the top one by PAGE-Net, is well known as one of the most associated pathways to GBM.[20] Survival models by both univariate and multivariate Cox regression analyses for the nine long non-coding RNAs (lncRNAs) in GBM identified the neuroactive ligand-receptor interaction pathway as the most related pathway.[21]

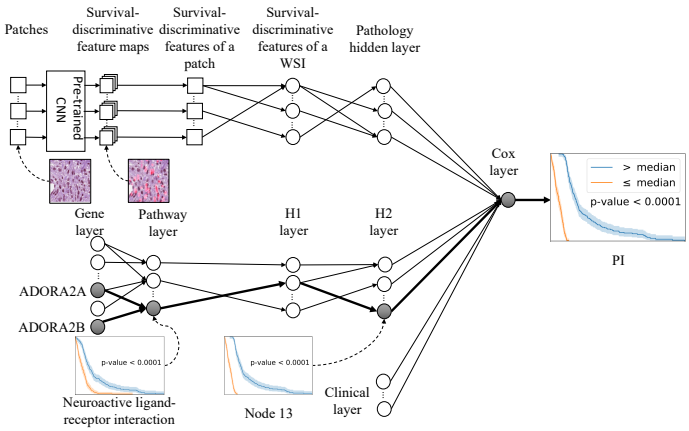

Fig. 5. Overview of the model interpretation

The axon guidance pathway harbored the top-ranked CNVs with respect to GBM.[22] The down-regulation of the endocytosis pathway was likely to be a common trait in glioma tumors.[23] For instance, the down-regulated differentially expressed genes (DEGs) associated with the glioma gene expression profile GSE4290, were enriched in the endocytosis pathway.[24] The collagen formation pathway enriched for the candidate genes, identified by weighted gene co-expression network analysis, with RNA sequencings of GBM patients from the Chinese Glioma Genome Atlas database.[25] Eighteen cytokines, which differentiated normal and GBM serum samples, were enriched in both of the cytokine-cytokine receptor interaction and Jak-STAT pathways.[26] Furthermore, over-expressed ADORA2A is one piece of evidence for high-grade gliomas given by the World Health Organization (WHO).[28] HTR7, enriched in the neuroactive ligandreceptor interaction pathway, was reported to contribute to diffuse intrinsic pontine glioma development and progression.[31] MET, well-known as an oncogene, has been revealed as a functional marker in Glioblastoma stem cells, since it benefits glioma invasiveness and self-reconstruction.[29]

Figure 5 shows the hierarchical biological mechanisms on both the histopathologcial images and genomic data in PAGE-Net. In the pathology-specific layers, morphological patterns, which are associated to patient survival, are scored by the survival-discriminative features, and the global features are introduced into the model. The survival-discriminative feature maps substantially capture the nuclei and nuclear debris of interest on a WSI. In the genome-specific layers, activated genes, including ADORA2A and ADORA2B, trigger the neuroactive ligand-receptor interaction pathway, and the pathway contributes patient survival in a non-linear manner with other pathways in the hidden layers. The Kaplan-Meier plots of the pathway and Node 13 in the H1 layer show the different survival distributions with the two groups separated by the median of the node values. The Node 13 values can be considered as a potential prognostic factor that can predict patient survival.

5. Conclusion

In this paper, we propose an integrative deep learning model (PAGE-Net) that captures both morphological patterns on histopathologcial WSIs, and pathway-based genetic mechanisms of a complex human cancer, while predicting cancer survival outcomes with histopatholog-

cial images and genomic data. PAGE-Net produced outstanding predictive performance and showed promising potential to identify genetic and histopathologcial prognostic factors simultaneously associated with patient survival. The survival-discriminative features identified by the pre-trained CNN were assessed by a pathologist, who determined that the features can identify nuclei and nuclear debris, which may be related to patient survival. The integrative deep learning model, PAGE-Net, also shows that data integration of the histopathologcial images and genomic data is essential for enhancing patient survival rates rather than analyses conducted with a single data type.

6. Acknowledgments

This research was supported by the Ministry of Science, ICT, Korea, under the High-Potential Individuals Global Training Program (2019–0–01601). supervised by the Institute for Information & Communications Technology Planning & Evaluation (IITP).

References

1. J. Cheng *et al.*, Integrative Analysis of Histopathological Images and Genomic Data Predicts Clear Cell Renal Cell Carcinoma Prognosis, *Cancer Research* **77**, e91 (2017).
2. X. Zhu *et al.*, Lung cancer survival prediction from pathological images and genetic data - An integration study, in *2016 IEEE 13th International Symposium on Biomedical Imaging (ISBI)*, 2016.
3. V. Popovici *et al.*, Joint analysis of histopathology image features and gene expression in breast cancer, *BMC Bioinformatics* **17**, p. 209 (2016).
4. N. P. Group, Histopathology is ripe for automation, *Nature Biomedical Engineering* **1**, p. 925 (2017).
5. D. Komura and S. Ishikawa, Machine Learning Methods for Histopathological Image Analysis, *Computational and Structural Biotechnology Journal* **16**, 34 (2018).
6. D. C. Cireşan *et al.*, Mitosis Detection in Breast Cancer Histology Images with Deep Neural Networks, in *Medical Image Computing and Computer-Assisted Intervention – MICCAI 2013*, 2013.
7. Y. Xu *et al.*, Deep Convolutional Activation Features for Large Scale Brain Tumor Histopathology Image Classification and Segmentation, in *2015 IEEE International Conference on Acoustics, Speech and Signal Processing (ICASSP)*, 2015.
8. M. G. Ertosun and D. L. Rubin, Automated Grading of Gliomas using Deep Learning in Digital Pathology Images: A modular approach with ensemble of convolutional neural networks, in *AMIA Annual Symposium Proceedings*, 2015.
9. L. Hou *et al.*, Automatic histopathology image analysis with CNNs, in *2016 New York Scientific Data Summit (NYSDS)*, 2016.
10. P. Mobadersany *et al.*, Predicting cancer outcomes from histology and genomics using convolutional networks, *Proceedings of the National Academy of Sciences* **115**, E2970 (2018).
11. X. Zhu, J. Yao, F. Zhu and J. Huang, WSISA: Making Survival Prediction from Whole Slide Histopathological Images, in *2017 IEEE Conference on Computer Vision and Pattern Recognition (CVPR)*, 2017.
12. D. Sun, L. Ao, T. bo and W. Minghui, Integrating genomic data and pathological images to effectively predict breast cancer clinical outcome, *Computer Methods and Programs in Biomedicine* **161**, 45 (2018).
13. J. Hao, Y. Kim, T. Mallavarapu, J. Oh and M. Kang, Cox-PASNet: Pathway-based Sparse

Deep Neural Network for Survival Analysis, in *Proceedings of IEEE International Conference on Bioinformatics & Biomedicine (IEEE BIBM 2018)*, 2018.
14. Z. Hu, T. Turki, N. Phan and J. T. L. Wang, A 3D Atrous Convolutional Long Short-Term Memory Network for Background Subtraction, *IEEE Access* **6**, 43450 (2018).
15. T. Guan and H. Zhu, Atrous Faster R-CNN for Small Scale Object Detection, in *2017 2nd International Conference on Multimedia and Image Processing (ICMIP)*, 2017.
16. T. Zhi, L.-Y. Duan, Y. Wang and T. Huang, Two-stage pooling of deep convolutional features for image retrieval, in *2016 IEEE International Conference on Image Processing (ICIP)*, 2016.
17. Y.-L. Boureau, J. Ponce and Y. Lecun, A Theoretical Analysis of Feature Pooling in Visual Recognition, in *27th International Conference on Machine Learning (ICML 2010)*, 2010.
18. J. Reimand *et al.*, Pathway enrichment analysis and visualization of omics data using g: Profiler, GSEA, Cytoscape and EnrichmentMap, *Nature Protocols* **14**, 482 (2019).
19. N. Simon, J. Friedman, T. Hastie and R. Tibshirani, Regularization Paths for Cox's Proportional Hazards Model via Coordinate Descent, *Journal of Statistical Software* **39**, 1 (2011).
20. J. Pal *et al.*, Abstract 2454: Genetic landscape of glioma reveals defective neuroactive ligand receptor interaction pathway as a poor prognosticator in glioblastoma patients, in *Proceedings of the American Association for Cancer Research Annual Meeting 2017*, Apr 2017.
21. B. Lei and ohters, Prospective Series of Nine Long Noncoding RNAs Associated with Survival of Patients with Glioblastoma, *J Neurol Surg A Cent Eur Neurosurg* **79**, 471 (2018).
22. M. Xiong *et al.*, Genome-Wide Association Studies of Copy Number Variation in Glioblastoma, in *2010 4th International Conference on Bioinformatics and Biomedical Engineering*, June 2010.
23. D. P. Buser *et al.*, Quantitative proteomics reveals reduction of endocytic machinery components in gliomas, *EBioMedicine* **46**, 32 (2019).
24. M. Liu *et al.*, The Identification of Key Genes and Pathways in Glioma by Bioinformatics Analysis, *J Immunol Res* **2017**, p. 1278081 (2017).
25. M. Liu *et al.*, Identification of survivalassociated key genes and long noncoding RNAs in glioblastoma multiforme by weighted gene coexpression network analysis, *International Journal of Molecular Medicine* **43**, 1709 (2019).
26. M. B. Nijaguna *et al.*, An Eighteen Serum Cytokine Signature for Discriminating Glioma from Normal Healthy Individuals, *PLoS One* **10**, p. e0137524 (2015).
27. M.-E. Halatsch *et al.*, Epidermal Growth Factor Receptor Pathway Gene Expressions and Biological Response of Glioblastoma Multiforme Cell Lines to Erlotinib, *Anticancer Res* **28**, 3725 (2008).
28. J. Huang *et al.*, Differential Expression of Adenosine P1 Receptor ADORA1 and ADORA2A Associated with Glioma Development and Tumor-Associated Epilepsy, *Neurochem Res* **41**, 1774 (2016).
29. C. Boccaccio and P. M. Comoglio, The MET Oncogene in Glioblastoma Stem Cells: Implications as a Diagnostic Marker and a Therapeutic Target, *Cancer Research* **73**, 3193 (2013).
30. J. Guo, A. V. Schally, M. Zarandi, J. Varga and P. C. Leung, Antiproliferative effect of growth hormone-releasing hormone (GHRH) antagonist on ovarian cancer cells through the EGFR-Akt pathway, *Reproductive Biology and Endocrinology* **8**, p. 54 (2010).
31. L. Deng *et al.*, Bioinformatics analysis of the molecular mechanism of diffuse intrinsic pontine glioma, *Oncology Letters* **12**, 2524 (2016).
32. D. Jantas *et al.*, An endogenous and ectopic expression of metabotropic glutamate receptor 8 (mGluR8) inhibits proliferation and increases chemosensitivity of human neuroblastoma and glioma cells, *Cancer Letter* **432**, 1 (2018).